Multiparameter Elastic Full Waveform Inversion for Reservoir Interpretation

Introduction

Full Waveform Inversion (FWI) has evolved to a robust and reliable technique to build accurate velocity models for depth imaging which has been routinely applied in seismic processing for both land and marine surveys. By incorporating more accurate physics, elastic FWI further enhances this capability, delivering highly precise models even in structurally complex regions with strong impedance contrasts such as salt boundaries (Macesanu *et al.*, 2024, Liu *et al*., 2025). FWI-derived reflectivity (FDR), computed as the directional derivative of the velocity model following high-frequency FWI, produces a high-resolution image comparable to least-squares RTM results. (Wang *et al*., 2021).

Conventional single-parameter elastic FWI focuses mainly on P-wave velocity inversion, with shear-wave velocity and density updated passively through analytical relationships linked to Vp, often calibrated using well information. Although this approach has proven robust and effective, in geological settings exhibiting Class IIp AVO anomalies, which are typically spatially localized, density often exhibits trends opposite to those of P- and S-wave velocities, such that a single empirical relationship cannot adequately represent the entire model.

Alternatively, multiparameter elastic FWI (MP-EFWI) simultaneously inverts for P-wave velocity and reflectively (Huang *et al*., 2025, Macesanu *et al*., 2025). In this approach, the elastodynamic equations are formulated in terms of velocities and P-wave reflectivity. Density is not a required parameter for modelling and inversion although its relative changes can be estimated from reflectivity, which is iteratively updated within the same FWI framework. To minimize the crosstalk between background velocity and reflectivity in our MP-EFWI framework, we applied an effective scale separation of the FWI gradient.

In this work, we apply MP-EFWI workflow to narrow-azimuth data containing a Class IIp AVO anomaly identified at a well location. Results show that both background velocity and reflectivity can be properly inverted, allowing the derivation of a relative density profile that agrees well with the well log, which demonstrates the potential of our MP-EFWI for reservoir interpretation.

Method

The multiparameter elastic FWI (MP-EFWI) utilizes the reformulated system of elastic wave equation in term of velocity and reflectivity as follows (Huang *et al*., 2025):

$$\begin{cases} \frac{\partial \tilde{v}_i}{\partial t} = \frac{\partial \sigma_{ij}}{\partial x_j} \\ \frac{\partial \sigma_{ij}}{\partial t} = \tilde{c}_{ijkl}\ \frac{\partial \tilde{v}_k}{\partial x_l} - \tilde{c}_{ijkl}\left(2r_l^p - \frac{1}{V_p}\frac{\partial V_p}{\partial x_l}\right)\tilde{v}_k \end{cases} \tag{1}$$

where $\tilde{v}_i$ $(i = 1,2,3)$ are the weighted particle velocity wavefield; σ_{ij} represent the stress tensor, $\tilde{c}_{ijkl}$ is the weighted stiffness tensor. In an isotropic case, the weighted stiffness tensor is given by

$$\tilde{c}_{ijkl} = \frac{1}{2}\left(V_p^2 - 2V_s^2\right)\delta_{ij}\delta_{kl} + V_s^2\left(\delta_{ik}\delta_{jl} + \delta_{il}\delta_{jk}\right), \tag{2}$$

where its components are functions of P- and S-wave velocity and independent of density. In anisotropic media, the weighted stiffness tensor components additionally depend on the Thompsen parameters.

In MP-EFWI, the inversion for velocity and reflectivity are performed by separating the FWI gradient into low- and high-wavenumber components using the scattering imaging condition (Whitmore and Crawley, 2012; Ramos-Martinez *et al*., 2016).

Field data example

We applied MP-EFWI to a narrow-azimuth streamer dataset acquired in deep-water offshore Brazil. The water depth ranges from approximately 1500 m to over 3000 m, with a rugose seabed. A Class IIp AVO anomaly was identified at one of the wells, where the reservoir interval exhibits increasing trends in both sonic and shear velocities, while density decreases, as shown in Figures 1a–1c. Data were acquired using a narrow-azimuth, 12-cable streamer configuration with 75 m cable spacing and a maximum inline offset of 8100 m.

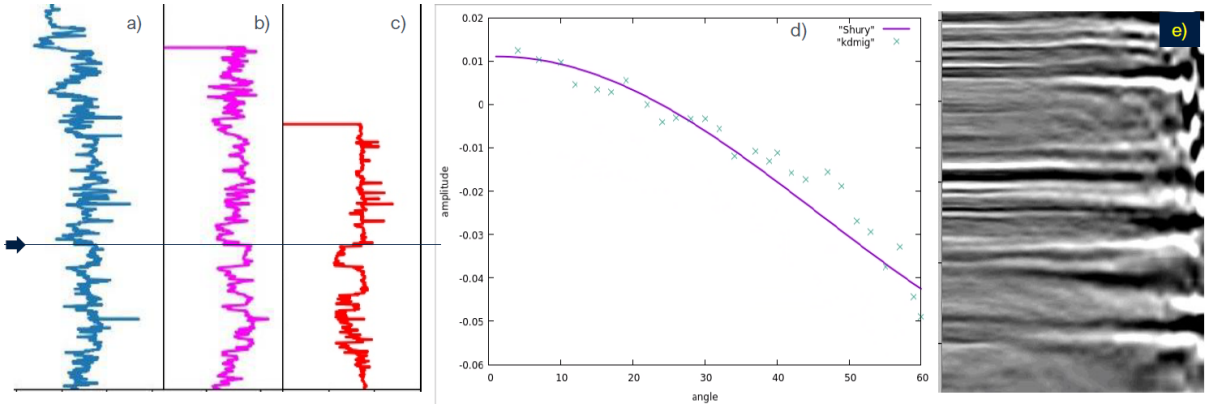

Figure 1: *a) Sonic, b) shear and c) density logs at a well location. The arrow points to the depth of the top reservoir where opposite trends occur; d) analytical reflection coefficient (solid line) computed from the wells-log information at the top of the reservoir; e) image gather at the well location showing phase reversal as angle increase; the extracted amplitudes displayed as x-markers in panel d), match the analytical reflection coefficient reasonably well.*

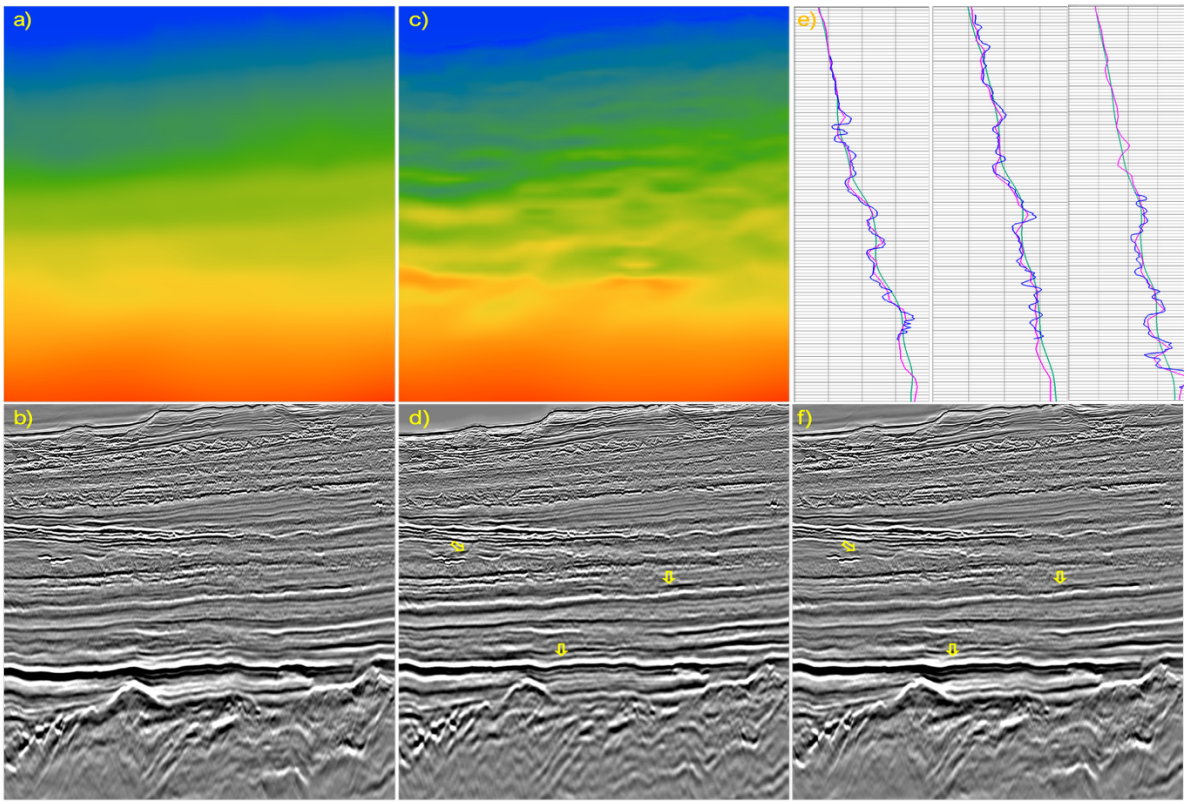

Figure 2. *a) Legacy model used as initial for MP-EFWI; b) RTM image computed from initial model; inverted a) velocity and b) reflectivity after 40 Hz MP-EFWI; e) filtered sonic log (blue) compared with profiles at three well-log locations for the initial (green) and inverted (pink) velocity; f) RTM image using the inverted velocity displayed in panel c).*

Before FWI, the input data was minimally pre-processed including denoising and debubble. Starting from a legacy model as the initial model, MP-EFWI was run staring at 6 Hz and progressively to 40 Hz jointly invert the P wave velocity (Vp) and the reflectivity. Figures 2a and 2b show, respectively, the initial velocity model and the corresponding 40 Hz RTM image using this model; Figures 2c and 2d show the inverted velocity model (Vp) and the reflectivity. Due to the scale separation, the inversion produces a background velocity model, and the high-resolution component yields the inverted reflectivity. Compared to the RTM image using the initial model, the inverted reflectivity (Figure 2d) has higher resolution and better focusing as pointed by the arrows. Reflectors beneath the high-impedance contrast associated with volcanic formations exhibit enhanced continuity and improved resolution. The inverted velocity model (Figure 2c) shows very good agreement with the filtered sonic log (Figure 2e) and yields more accurate kinematics, as supported by the improved RTM image in Figure 2f compared with that obtained using the initial model (Figure 2b). Figure 3 presents a comparison between a depth slice of the RTM image (Figure 3a) and the corresponding inverted reflectivity (Figure 3b), which demonstrates the superior resolution achieved in the reflectivity image and a significant acquisition footprint mitigation. Moreover, MP-EFWI utilized only one-third of the shots required by RTM.

From the inverted velocity and reflectivity, the relative impedance and consequently the relative density can be derived as shown in Figure 4a. In Figure 4b, we compare the relative density log (red) with the one derived (blue) from the inverted velocity and reflectivity at the well location as shown in Figure 1. Clearly, the multiparameter elastic FWI overcomes the challenges and successfully represent the case of AVO anomaly.

Conclusions

MP-EFWI exploits a reformulated elastic wave-equation system to jointly invert P-wave velocity and reflectivity in elastic media, providing a foundation for deriving additional reservoir attributes. Our approach separates the FWI gradient into low- and high-wavenumber components to update the background velocity and high-resolution reflectivity, respectively, effectively mitigating parameter crosstalk. Results from narrow-azimuth data acquired in Brazil, demonstrate is possible to identify negative correlation between velocity and density at a potential target where a Class IIp AVO anomaly has been identified. In addition, the iterative updating of reflectivity provides enhanced seismic imaging compared with conventional imaging.

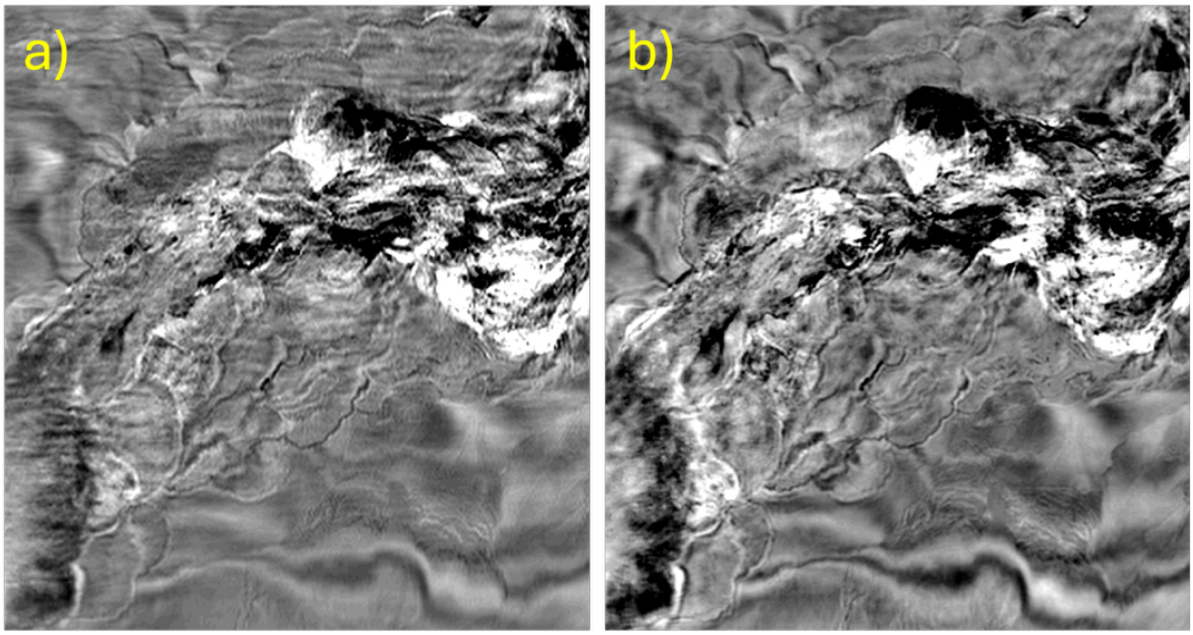

Figure 3. *Depth slices for the a) RTM image and b) inverted reflectivity using our MP-EFWI approach.*

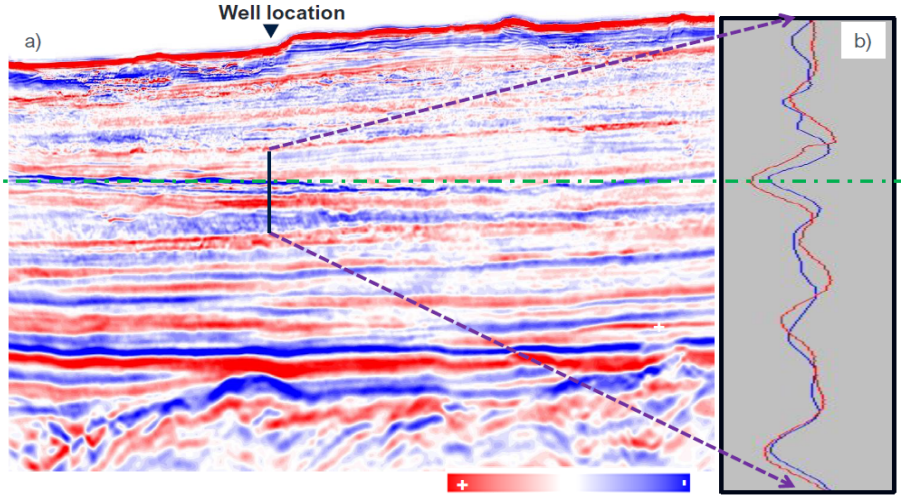

Figure 4. *a) Relative density derived from the inverted velocity and reflectivity by MP-EFWI; b) filtered relative density log (red) compared with the derived relative density (blue) at the well location. The negative density contrast at the target reservoir depth (highlighted by the green line) is successfully resolved by the MP-EFWI approach.*

Acknowledgements

We thank our colleagues Alejandro Alcudia-León, Yermek Balabekov, Zhijian Luo and Cristina Reta-Tang for their assistance in the field data preparation and valuable discussions. We are grateful to TGS for permission to publish this work and TGS Multiclient for the permission to use the data examples.

References

Huang, G., C. Macesanu, F. Liu, J. Ramos-Martínez, D. Whitmore, and Calderón, C. [2025]. Multiparameter elastic FWI for joint inversion of velocity and reflectivity: 86th EAGE Conference & Exhibition, *Extended Abstracts*.

Liu, F., C. Macesanu, H. Xing, M. Romanenko, G. Zhan, C. Calderón-Macías and Wang, B. [2025]. Elastic full-waveform inversion: Enhance imaging for legacy and modern acquisition: *The Leading Edg*e, **44**, 5, 338-343.

Macesanu, C., G. Huang, F. Liu, J. Ramos-Martínez, and Whitmore, D. [2025]. Elastodynamic modelling and inversion with reflectivity terms.

Ramos-Martínez, J., S. Crawley, K. Zou, A.A. Valenciano, L. Qiu, and Chemingui, N. [2016]. A robust gradient for long wavelength FWI updates: 78th EAGE Conference & Exhibition, *Extended Abstracts*.

Wang, B., Y. He, J. Mao, F. Liu, Hao, M. Perz, and Mitchel, S. [2021]. Inversion-based imaging: LSRTM to FWI Imaging*: First Break*, **39**(12), 85-93.

Whitmore, N.D. and Crawley, S. [2012]. Applications of RTM inverse scattering imaging conditions: 82nd SEG Annual International Meeting, SEG, *Expanded Abstracts*, 1-2.